Biol Cell (1995) 83, 105–120

Original article

Cellular effects of olomoucine, an inhibitor of cyclin-dependent kinases

RT Abraham [a], M Acquarone [b], A Andersen [b], A Asensi [b], R Bellé [c], F Berger [d], C Bergounioux [e], G Brunn [a], C Buquet-Fagot [f], D Fagot [f], N Glab [e], H Goudeau [b], M Goudeau [b], P Guerrier [g], P Houghton [h], H Hendriks [i], B Kloareg [b], M Lippai [g], D Marie [b], B Maro [i], L Meijer [b] *, J Mester [f], O Mulner-Lorillon [c], SA Poulet [b], E Schierenberg [k], B Schutte [l], D Vaulot [b], MH Verlhac [j]

[a] *Mayo Clinic, Department of Immunology, Rochester, MI 55905, USA;*
[b] *CNRS, Station Biologique, BP 74, 29680 Roscoff;*
[c] *Université Paris VI, Laboratoire de Physiologie de la Reproduction, 9, quai Saint-Bernard, 75005 Paris;*
[d] *Marine Biological Association, The Laboratory, Citadel Hill, Plymouth PL1 2PB, UK;*
[e] *Université de Paris-Sud, Laboratoire de Physiologie Végétale Moléculaire, Bâtiment 430, 91405 Orsay Cedex;*
[f] *INSERM, Unité U55, Centre de Recherches Paris-Saint-Antoine, 184, rue du Faubourg-Saint-Antoine, 75571 Paris Cedex 12;*
[g] *École Normale Supérieure, Laboratoire de Biologie Moléculaire et Cellulaire, 46, allée d'Italie, 69364 Lyon Cedex 07, France;*
[h] *Department of Biochemical and Clinical Pharmacology, St Jude Children's Research Hospital, 332 North Lauderdale, PO Box 318, Memphis, TN 38101-0318, USA;*
[i] *New Drug Development Office, Free University Hospital, Gebouw Zuid, Amstelveenseweg 601, Postbox 7057, 1007 MB Amsterdam, the Netherlands;*
[j] *Institut Jacques-Monod, Université Paris VII, Tour 43, 2, place Jussieu, 75251 Paris Cedex 05, France;*
[k] *Zoologisches Institut der Universität Köln, Weyertal 119, 5000 Köln 41, Germany;*
[l] *University of Limburg, Faculty of Medicine, Department of Molecular Cell Biology and Genetics, Universiteitssingel 50, PO Box 616, 6200 MD Maastricht, the Netherlands*

(Received 24 April 1995; accepted 9 June 1995)

Summary – Olomoucine (2-(2-hydroxyethylamino)-6-benzylamino-9-methylpurine) has been recently described as a competitive inhibitor (ATP-binding site) of the cell cycle regulating $p34^{cdc2}$/cyclin B, $p33^{cdk2}$/cyclin A and $p33^{cdk2}$/cyclin E kinases, the brain $p33^{cdk5}$/p35 kinase and the ERK1/MAP-kinase. The unusual specificity of this compound towards cell cycle regulating enzymes suggests that it could inhibit certain steps of the cell cycle. The cellular effects of olomoucine were investigated in a large variety of plant and animal models. This compound inhibits the G1/S transition of unicellular algae (dinoflagellate and diatom). It blocks *Fucus* zygote cleavage and development of *Laminaria* gametophytes. Stimulated *Petunia* mesophyl protoplasts are arrested in G1 by olomoucine. By arresting cleavage it blocks the development of *Calanus* copepod larvae. It reversibly inhibits the early cleavages of *Caenorhabditis elegans* embryos and those of ascidian embryos. Olomoucine inhibits the serotonin-induced prophase/metaphase transition of clam oocytes; furthermore, it triggers the release of these oocytes from their meiotic metaphase I arrest, and induces nuclei reformation. Olomoucine slows down the prophase/metaphase transition in cleaving sea urchin embryos, but does not affect the duration of the metaphase/anaphase and anaphase/telophase transitions. It also inhibits the prophase/metaphase transition of starfish oocytes triggered by various agonists. *Xenopus* oocyte maturation, the *in vivo* and *in vitro* phosphorylation of elongation factor EF-1 are inhibited by olomoucine. Mouse oocyte maturation is delayed by this compound, whereas parthenogenetic release from metaphase II arrest is facilitated. Growth of a variety of human cell lines (rhabdomyosarcoma cell lines Rh1, Rh18, Rh28 and Rh30; MCF-7, KB-3-1 and their adriamycin-resistant counterparts; National Cancer Institute 60 human tumor cell lines comprising nine tumor types) is inhibited by olomoucine. Cell cycle parameter analysis of the non-small cell lung cancer cell line MR65 shows that olomoucine affects G1 and S phase transits. Olomoucine inhibits DNA synthesis in interleukin-2-stimulated T lymphocytes (CTLL-2 cells) and triggers a G1 arrest similar to interleukin-2 deprivation. Both cdc2 and cdk2 kinases (immunoprecipitated from nocodazole- and hydroxyurea-treated CTLL-2 cells, respectively) are inhibited by olomoucine. Both yeast and *Drosophila* embryos were insensitive to olomoucine. Taken together the results of this Noah's Ark approach show that olomoucine arrests cells both at the G1/S and the G2/M boundaries, consistent with the hypothesis of a prevalent effect on the cdk2 and cdc2 kinases, respectively.

cell cycle / proliferation / protein kinases / cyclin-dependent kinases / cdc2 / cdk1 / cdk2 / olomoucine / purines / 2-(2-hydroxyethylamino)-6-benzylamino-9-methylpurine

* Correspondence and reprints

Abbreviations: BrdU, bromo-deoxyuridine; cdc, cell division cycle; cdk, cyclin-dependent kinase; GVBD, germinal vesicle breakdown; IL-2, interleukin-2; MAP kinase, mitogen-activated protein kinase; MPF, M-phase promoting factor; NSW, millipore-filtered natural sea water; PBS, phosphate-buffered saline; PI, propidium iodide.

Introduction

Virtually all cellular control mechanisms involve modifications in the covalent binding of phosphate groups to serine, threonine and tyrosine residues of proteins by protein kinases. The importance of protein kinases in all physiological processes has stimulated an active search for specific inhibitors of potential pharmacological interest [17]. Cyclin-dependent kinases (cdks) have recently raised considerable interest in view of their essential role in cell division cycle regulation [40, 55]. Cdks are catalytic subunits of protein kinases that associate with regulatory subunits, cyclins. Seven human cdks have been described so far [31, 32, 59]: cdk1 (= cdc2), cdk2, cdk3, cdk4, cdk5, cdk6 and cdk7. With the exception of cdk3, for which the regulatory cyclin has not yet been identified [59], all these cdks are regulated by the transient association with one member of the cyclin family: cyclin A (cdc2, cdk2), B1–B3 (cdc2), D1–D3 (cdk2, cdk4, cdk5, cdk6), E (cdk2 and cdk7). Cell cycle progression is thought to be regulated by such cdk complexes: G1/S transition (cdk2/cyclin E, cdk3/unknown cyclin, cdk4/cyclin D1-D3, cdk6/cyclin D3), S phase (cdk2/cyclin A), G2 (cdc2/cyclin A), G2/M transition (cdc2/cyclin B). Other cdc2-related kinases have been sequenced which await identification of their regulatory partners and their cell cycle regulatory functions [31].

Increasing data support the importance of cdk's deregulation in human tumor development (for review see [35]). Recently, natural inhibitors of cyclin-dependent kinases, such as $p16^{INK4}$ (inhibitor of cdk4/cyclin D1-D3) [19, 41, 53] and $p21^{CIP1, SDI1, WAF1}$(a general inhibitor of cdks) [7, 13, 15, 42, 63], have been presented as tumor suppressors directly implicated in the causes of cancer. The frequent deregulation of cdks and their natural inhibitors in cancer stimulates an active search for chemical inhibitors of cdks. We have therefore designed a simple, mechanism-based assay using affinity-purified $p34^{cdc2}$/cyclin B kinase as a screening target for new anti-mitotic compounds of potential anti-tumor interest [47].

While investigating the inhibitory action of purine derivatives on the $p34^{cdc2}$/cyclin B kinase, we discovered a compound with high specificity, olomoucine (2-(2-hydroxyethylamino)-6-benzylamino-9-methylpurine) [62]. This compound acts as a competitive inhibitor for ATP binding. Among 35 purified kinases tested, only cdc2, cdk2, cdk5 and erk1, but not cdk4 and cdk6, were found to be substantially inhibited by micromolar concentrations of olomoucine. Olomoucine is related to the previously described cdc2 inhibitors 6-dimethylaminopurine [29, 39] and N^6-(Δ^2-isopentenyl)adenine [47], but not to the recently discovered cdc2 inhibitor butyrolactone-I ([21, 56]; for a review on chemical inhibitors of cdks, see [26]).

The cellular effects of olomoucine have been investigated in this work using a variety of cellular models ranging from unicellular algae to human tumor cells. Olomoucine was found to inhibit cell proliferation both at the G1/S and G2/M boundaries. These results are consistent with the hypothesis of a prevalent *in vivo* effect on cdk2 and cdc2, respectively. By its unique selectivity, olomoucine provides an anti-mitotic reagent which preferentially inhibits certain steps of the cell cycle and may constitute a lead compound for the design of new anti-tumor agents.

Materials and methods

Chemicals

Olomoucine, 2-(2-hydroxyethylamino)-6-benzylamino-9-methylpurine) was obtained from ACDC Research Laboratory and dissolved at 100 mM in dimethylsulfoxide. 8-hydroxyeicosatetraenoic acid was a generous gift of Dr A Brash (Vanderbilt University, Nashville, TN, USA). 1-Methyladenine and doxorubicin were obtained from Sigma Chemicals.

Dinoflagellate and diatom

Amphidinium carterae strain CCMP1314 (Dinophyceae) and *Thalassiosira weissflogii* strain CCMP1336 (Bacillariophyceae) originated from the Provasoli-Guillard Center for Culture of Marine Phytoplancton (Bigelow Laboratory for Ocean Sciences, West Boothbay Harbor, Maine, USA) and were maintained in exponential growth in batch cultures at 20°C at a light intensity of about 100 μE/ms in potassium-enriched seawater medium [20].

Cultures were placed in total darkness for 36 h to induce cell cycle arrest with a reduction in the number of S phase cells [60] before addition of olomoucine. A blank and a control with DMSO were also included. Cultures were put back in continuous light just after addition of olomoucine. Due to difference in the blocking dynamics between the two species [60], sampling was carried out after 0, 2, 4, 6, 8, 9, 10, 11, 12, 14, 16 h for *A carterae* and 0, 1, 2, 3, 4, 5, 6, 7, 8, 10, 12 h for *T weissflogii*.

Nuclear DNA was stained with 4',6-diamidino-2-phenylindole (DAPI) using a modification of the Otto procedure [44]. At each sampling time, 0.5 ml of culture was centrifuged for 10 min at 2000 *g* and cells were resuspended in 1 ml of a solution of 0.2 M citric acid and 0.1% Triton X-100, incubated at 20°C for 1 h and stored at 4°C for a maximum of 24 h. Just before analysis, samples were centrifuged for 20 min at 8000 *g*. The supernatant was eliminated and the cells were resuspended in 100 μl of 0.2 M citric acid and 0.1% Triton X-100 to which 400 μl of 0.4 M Na_2HPO_4 and 0.5 μg DAPI/ml were added.

Cell DNA fluorescence was measured with an EPICS 541 flow cytometer (Coulter, Hialeah, FL, USA) equipped with an argon laser (Coherent, Palo Alto, CA, USA) set for emission at 357 nm, a Biosense flow cell and a confocal lens to increase sensitivity [43, 61]. DNA histograms were analyzed to obtain the percentage of cells in each cell cycle phase using Multicycle (Phoenix Flow Systems, San Diego, CA, USA).

Fucus spiralis zygotes

Zygotes of *Fucus spiralis* undergo the first cell division cycle within 22 h after fertilization. Before the first division they polarise according to various environmental gradients [22]. Photopolarisation has been used for these experiments. It is expressed by the rhizoid, a protrusion which develops on the side away from the prevailing light source. Cell division subsequently occurs perpendicular to the polarity axis.

Laminaria digitata gametophytes

Fertile sporophytes of *Laminaria digitata* were collected at Roscoff. Mature sori were cleaned, excised, rinsed several times with sterile seawater and cut in thin lamellae. Sorus slices were incubated in 50 ml Petri dishes in the presence of Provasoli-enriched seawater. Culture of zoospores was carried out at 12–13°C with a 18:8 light:darkness photoperiod, under 40 W cool-white fluorescent light at an approximate photon fluence rate of 20 μmol/m^2/s. Gametophytes were grown in the presence of various concentrations of olomoucine delivered when zoospores had settled onto the substratum and before the first cell division of gametophytes. Cultures were monitored weekly.

Petunia hybrida protoplasts

Mesophyll protoplasts were isolated from 4th to 6th leaves (numbered from the cotyledons to the apex) of *Petunia hybrida* (hybrid F1PxPC6, Dr Cornu, INRA, Dijon). Protoplasts (10^5/ml) were cultured under constant light at 26°C as described previously [3]. Olomoucine (1–200 μM) was added for 24 h to the *Petunia* cultures 14 h after their isolation. In some cases protoplasts were washed and resuspended in conditioned medium for

another 10 h. For cell cycle analysis nuclei were isolated from the protoplasts in Galbraith buffer [8], fixed in 1% formaldehyde (37%) and stained with 2 μg/ml of bisbenzimide Hoescht 33342. Cytometric analysis was performed on 2×10^4 nuclei with an EPICS V flow cytometer (Coulter) [45)].

Caenorhabditis elegans embryos

Caenorhabditis elegans embryos were cultivated as described previously [49]. To facilitate access of olomoucine, the egg envelope was fenestrated with a laser microbeam [50]. The timing, sequence and polarity of early cleavages, starting from the 2-cell stage embryo (AB) up to the primordial germcell P4 at the 24-cell stage, were examined under Nomarsky phase contrast.

Calanus helgolandicus embryos

The copepods *Calanus helgolandicus* were obtained by dredging in coastal waters in the Roscoff area. Freshly spawned eggs (20–30 per batch) were incubated, at constant temperature (14.5 ± 0.5°C), in Millipore-filtered sea water (500 μl), supplemented with olomoucine at various concentrations. Experiments were repeated three times. The extent of embryonic development was assessed by scoring the rate of hatching after 30 h incubation. Light microscopy examinations of hatched nauplii and embryos of the same age were performed under Nomarsky phase contrast and fluorescence (Hoescht 33342 staining) as described in [46].

Ruditapes philippinarum oocytes

Four- to five-year-old *Ruditapes philippinarum* clams were obtained from various commercial sources in the 'Golfe du Morbihan' and kept in running seawater. Oocytes were obtained by mincing the gonad with scissors in artificial seawater buffered at pH 8.0-8.2 with 2 mM Tris [54]. The suspension was filtered through cheesecloth and the oocytes were further washed three to four times and diluted to a 0.5% suspension. Only batches showing less than 5% spontaneous maturation were used. Oocyte maturation was triggered with serotonin (5-hydroxytryptamine), prepared freshly as a 10 mM stock solution. Germinal vesicle breakdown (GVBD) was scored 60 min after hormone addition. Metaphase-arrested oocytes were exposed to olomoucine and observed under fluorescence following Hoescht 33342 staining.

Marthasterias glacialis oocytes

Starfish oocytes were prepared as previously described [30] and maturation was induced by 1-methyladenine (1 μM) or 8-hydroxyeicosatetraenoic acid (1 μM). The effects of olomoucine on the prophase/metaphase transition were tested as described [62]. The hormone-dependent period was determined by exposure of an oocyte suspension to 1 μM 1-methyladenine and rapid transfer at various times of 50 μl aliquots to 12 ml of seawater, followed by determination of the percentage of GVBD 30 min later [30].

Sphaerechinus granularis embryos

Sea urchins were collected by diving in Brittany and kept in running seawater until use. Shedding of gametes was induced by injection of 0.2 ml of 0.2 M acetylcholine. Sperm was collected 'dry' and kept undiluted at +4°C. Eggs were collected in Millipore-filtered natural seawater (NSW). They were washed once with NSW and resuspended as a 10% (v/v) suspension. To facilitate fertilization membrane elevation, 0.1% (w/v) glycine was added to the egg suspension prior to fertilization. Sperm was diluted just before insemination (1 drop 'dry' sperm/5 ml NSW; 1 drop of this dilution/10 ml egg suspension). At 2–3 min after sperm addition the eggs were checked for successful fertilization (100% in all experiments) and the excess sperm was removed by washing the eggs once with NSW. All experiments were performed at +20°C.

Olomoucine was added 60 min after fertilization. Embryos were scored for cleavage under the microscope and examined after fixation and clearing. 200 μl egg suspension aliquots were injected at regular intervals in ethanol:chloroform:acetic acid (6:3:1). After 1 h the supernatant was removed and 1 ml fresh fixative was added. After another hour 200 μl glycerol 25% (v/v) was added, followed 1 h later by 200 μl glycerol 50% (v/v). Just before observation under the microscope (Nomarski phase contrast) acetic carmine was added to the eggs on the observation slide (1 vol stain/1 vol eggs) [29].

Phallusia mammillata embryos

Ripe ascidians were collected in Brittany and maintained under circulating seawater. Gametes were collected as previously described [11]. Inseminations were carried out in NSW and embryos exposed to olomoucine either 7 or 30 min after fertilization.

Xenopus laevis oocytes

Xenopus laevis oocytes were prepared as described previously [37]. Olomoucine was added together with 1 μM progesterone. *In vivo* phosphorylation of elongation factor 1 subunits β, γ and δ was assessed after immunoprecipitation of the whole complex [37] in ^{32}P-labelled oocytes.

Mouse oocytes

Mouse oocytes were prepared and cultured as described previously [23, 25].

Rhadomyosarcoma cell lines

Four cell lines derived from childhood rhabdomyosarcoma were used to evaluate the cytostatic activity of olomoucine *in vitro*. Lines Rh18, Rh 28 and Rh30 each demonstrated the t(2:13) rearrangement characteristic of alveolar type RMS and Rh 1 is representative of embryonal RMS. Lines Rh18, Rh 28 and Rh30 have been described previously [6, 16]. All cell lines were routinely grown in RPMI 1640 medium (Whittaker, Walkersville, MD) supplemented with 2 mM glutamine and 10% fetal calf serum (Hyclone, Logan, UT), without antibiotics. Logarithmically growing cells were harvested and plated at the following number per 35 mm well of a 6-well culture dish (Becton Dickinson, Lincoln Park, NJ): Rh1 at 3×10^3, Rh18 at 5×10^4, Rh28 at 3×10^5 and Rh30 at 4×10^4. Cells were allowed to attach overnight, and then exposed to olomoucine (0.1 to 300 μM) for 7 days. For Rh1 and Rh30 cells, colonies were enumerated, after air drying the plates and staining with crystal violet, using an ARTEK model 880 counter. For Rh18 and Rh28 cultures, which do not form discrete colonies, cell nuclei were determined using a Coulter counter after lysis of cells [5].

MCF-7 / MCF-7mdr and KB-3-1 / KB-A cell lines

The human breast cancer cell line MCF-7 and the derived MCF-7mdr adapted for growth in the presence of adriamycin (doxorubicin) [4] were obtained from Dr F Calvo, St Louis Hospital, Paris. The human epidermoid cancer cell lines KB-3-1 and the subline KB-A (adriamycin-resistant) [48] were obtained from Dr S Chevillârd, (Institut Curie, Paris). These cell lines were grown in Dulbecco-modified Eagle's medium (DMEM) supplemented with 10% fetal calf serum (Gibco). Adriamycin (1 μg/ml) was added to the MCF-7mdr and KB-A cells after passaging. For [^{3}H]thymidine incorporation experiments, cells were seeded in 24-well plates (50000/well) in the complete medium (without adriamycin). The next day, olomoucine was added at various concentrations in fresh medium. After 48 h of culture in the presence of olomoucine, [^{3}H]thymidine (2 μCi/ml) incorporation was evaluated by 30 min pulses. Radioactivity incorporated into insoluble material in 5% trichloracetic acid was measured by liquid scintillation counting. The data shown are means ± SEM of triplicates.

NCI disease-oriented in vitro screen

Sixty human tumor cell lines comprising nine tumor types [12] were cultured for 24 h prior to a 48 h continuous exposure to 0.01–100 μM olomoucine. A sulforhodaminine B protein assay was used to estimate the cytotoxicity.

Non-small cell lung cancer cell line MR65

The non-small cell lung cancer cell line MR65 was grown as monolayer culture in HEPES buffered Eagle's modified minimal essential medium (EMEM) supplemented with 10% newborn calf serum (Gibco), 1% L-glutamine (Serva), 1% non-essential amino acids (AUV, Cuyck, the Netherlands). The MR65 Cell line was a kind gift of Dr Gropp (Marburg, Germany).

Exponentially growing cell cultures were pulse-labeled with 10 μM BrdU for 30 min. Cells were rinsed twice with pre-warmed phosphate-buffered saline (PBS) and chased in culture medium supplemented with 5 μM deoxythymidine and various concentrations of olomoucine. After various periods of time cultures were harvested by trypsination, fixed in 70% cold ethanol and kept at 4°C in the dark.

Samples were stained as described previously [52]. Briefly, approximatively 10^6 cells were rinsed in PBS and the pellet was incubated in 0.4 mg/ml pepsin in 0.1 N HCl for 30 min at room temperature. After centrifugation at 400 *g* the pellet was resuspended in 2 N HCl and incubated for 30 min at 37°C. The isolated nuclei were rinsed in 0.1 M sodium tetraborate (pH 8.5) and 1 mg BSA in PBS (pH 7.4) and incubated with appropriately diluted monoclonal anti-BrdU antiserum (clone IIB5). After 1 h of incubation at room temperature in the dark, the nuclei were rinsed twice in BSA/PBS and antibody binding was visualized by

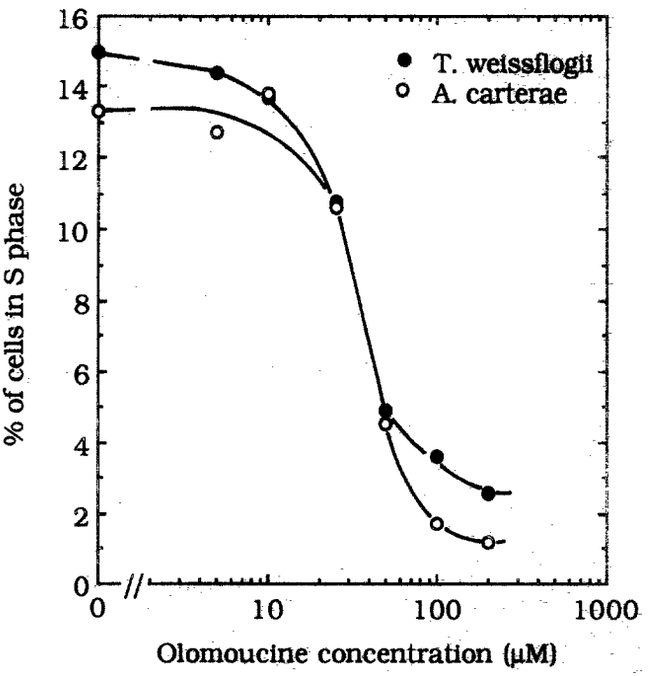

Fig 1. Olomoucine inhibits the G1/S transition of diatom and dinoflagellate. Cultures of the diatom *Thalassiosira weissflogii* and the dinoflagellate *Amphidinium carterae* were synchronized by exposure to darkness prior to light stimulation in the presence of increasing concentrations of olomoucine. Cells were analyzed by flow cytometry and the percent of S phase cells was plotted as a function of olomoucine concentration.

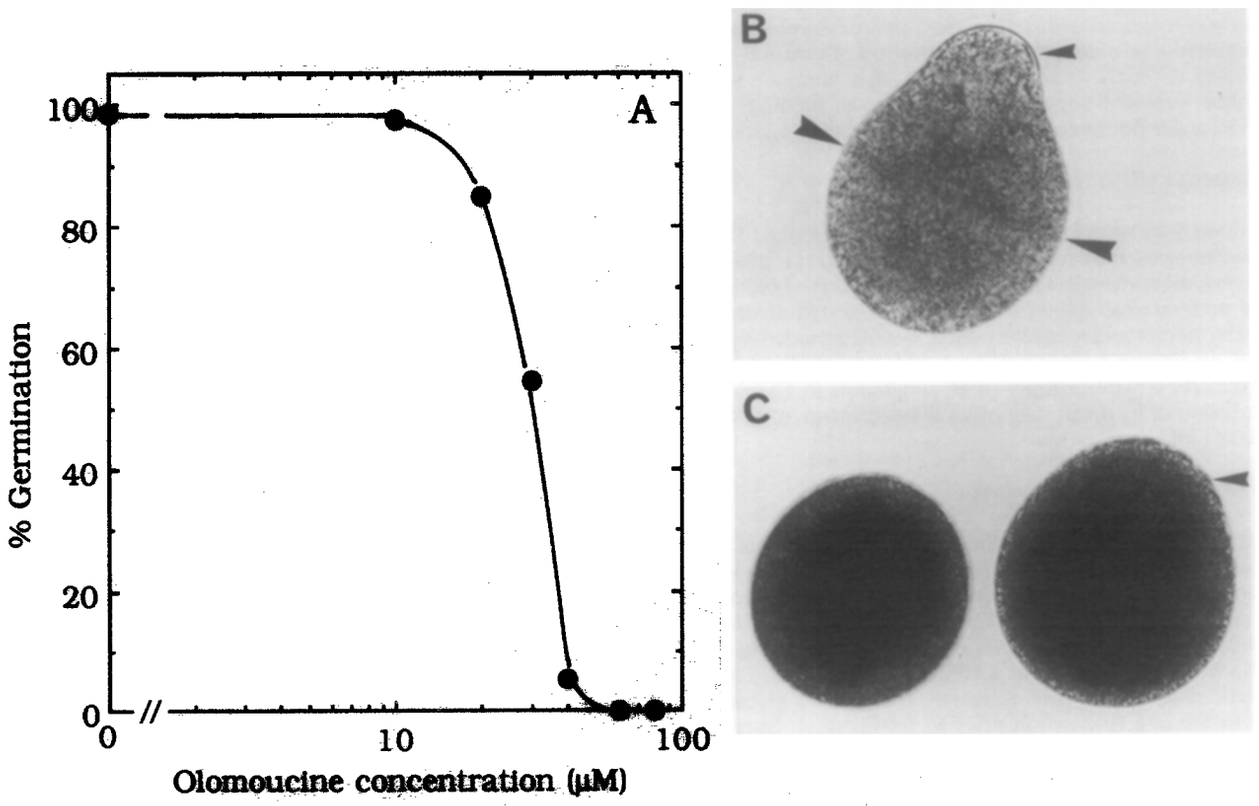

Fig 2. Olomoucine inhibits the early development of *Fucus* embryos. *Fucus* eggs were fertilized and exposed to various concentrations of olomoucine. **A.** Percentage of germination as a function of olomoucine concentration. **B.** Control germinated embryo; small arrow indicates the rhizoid; large arrows indicate the cleavage furrow. **C.** Two olomoucine-treated embryos; no cleavage has occurred, though one embryo has developed a rhizoid.

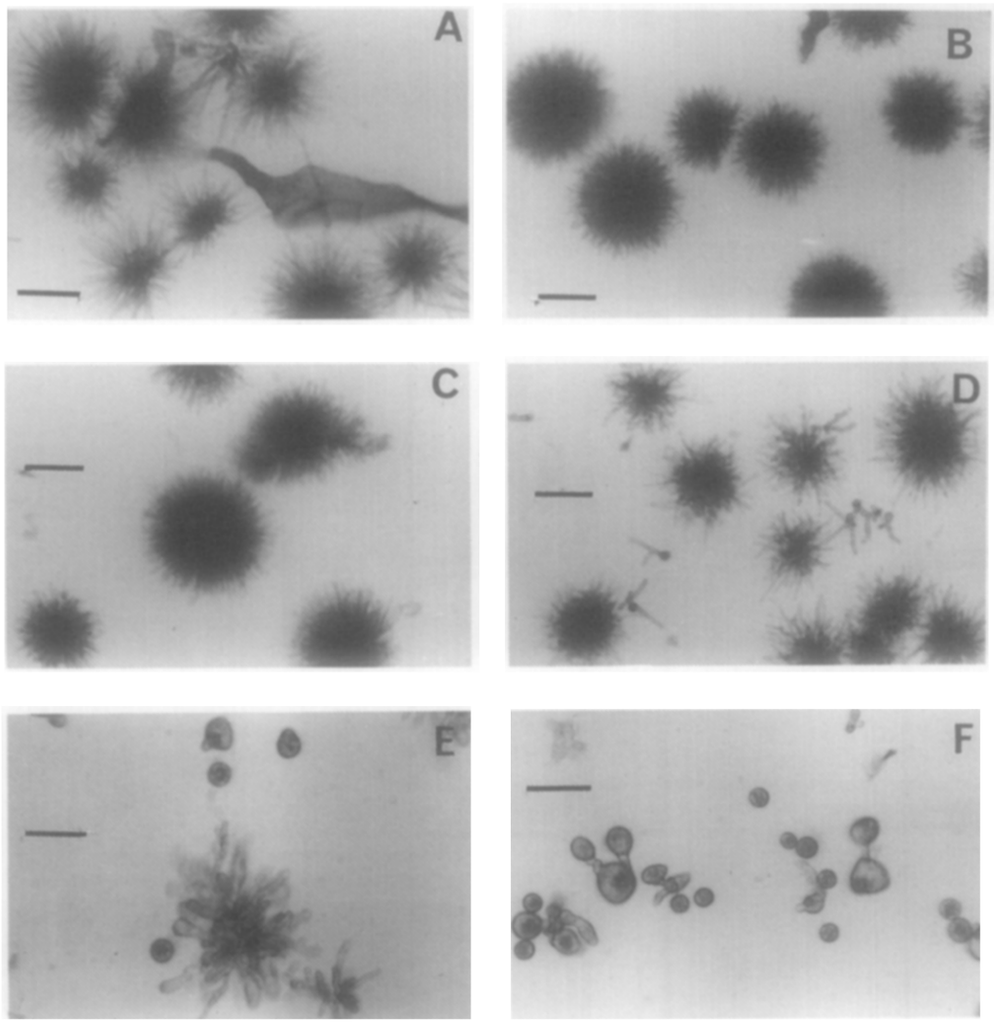

Fig 3. Olomoucine inhibits the early development of *Laminaria* gametophytes. 50-day-old gametophytes cultured in the absence **(A)** or presence of 3 μM **(B)**, 12.5 μM **(C)**, 25 μM **(D)**, 50 μM **(E)** or 50 μM **(F)** olomoucine. Bars represent 100 μm **(A–D)** or 25 μm **(E, F)**.

incubating the nuclei with FITC-conjugated rabbit anti-mouse Ig (Dako, Glostrup, Denmark) for 45 min at room temperature in the dark. Finally the nuclei were rinsed twice in BSA/PBS and resuspended in 0.5 ml cold PBS/propidium iodide (PI) 20 μg/ml, RNAse 100 μg/ml. After 15 min incubation the samples were ready for flow cytometric analysis on a FACSort (Becton Dickinson) equipped with a single air cooled Argon ion laser. The exciting light was 488 nm and the emission filters were 515–545 BP (green, FITC), 572–588 BP (orange) and 600 lp (red; PI). A minimum of 10000 cells per sample were stored in list mode. FITC signals were recorded as linear amplified data. For bivariate BrdU/PI analysis no compensation was used. Data analysis was performed with the standard Lysis and Cell-fit software. As a standard procedure for all analyses, data were gated on pulse processed PI signals to exclude doublets and larger aggregates.

From dotplots of PI *vs* log-FITC five compartments were identified from which five parameters reflecting the modes of cell progression through the cell cycle were determined [18]: 1) relative movement (RM) [2], mean DNA content of BrdU-positive undivided population normalized to G1 and G2 position; 2) fraction of undivided cells among the BrdU-positive population (F^+ undivided); 3) BrdU-negative G2 fraction ($F_{G2}-$); 4) BrdU-negative G1 fraction ($F_{G1}-$); and 5) the position of negative cells excluding the initial G2 cells normalized to G1 position. Means of the five parameters were plotted as a function of time after BrdU pulse labeling for each dose of olomoucine. To quantitatively assess the cell cycle progression, linear portions of the kinetic curves were fitted by linear regression analysis. For the BrdU-negative G1 and G2 fractions the linear regression analysis was performed on the logarithmically transformed data. The slopes of the regression lines were used to elucidate the changes in the rate of cell cycle progression.

Interleukin-2-stimulated T lymphocytes

CTLL-2 cells were cultivated as described previously [33] and treated with 50 units interleukin-2 (IL-2)/ml. [^{3}H]thymidine incorporation was evaluated as described previously [33]. Cell cycle data were obtained from cells which were treated for 14 h with olomoucine (100 μM) or, alternatively, were withdrawn from IL-2 for 12 h to induce G1 arrest prior to restimulation with IL-2 in the presence or absence of 100 μM olomoucine. Cells were fixed in ethanol and processed as described [33]. Fluorescence of PI-stained DNA was quantitated with a FACStar Plus flow cytofluorometer equipped with Lysis II software (Becton-Dickinson, San Jose, CA).

Cdc2 and cdk2 kinase assays were performed in duplicates using immunoprecipitates from nocodazole (14 h, 500 ng/ml), and hydroxyurea (14 h, 0.8 M), treated CTLL-2 cells, respectively, as previously described [34]. In either case olomoucine was added to the immunoprecipitates in 20 μl of kinase buffer.

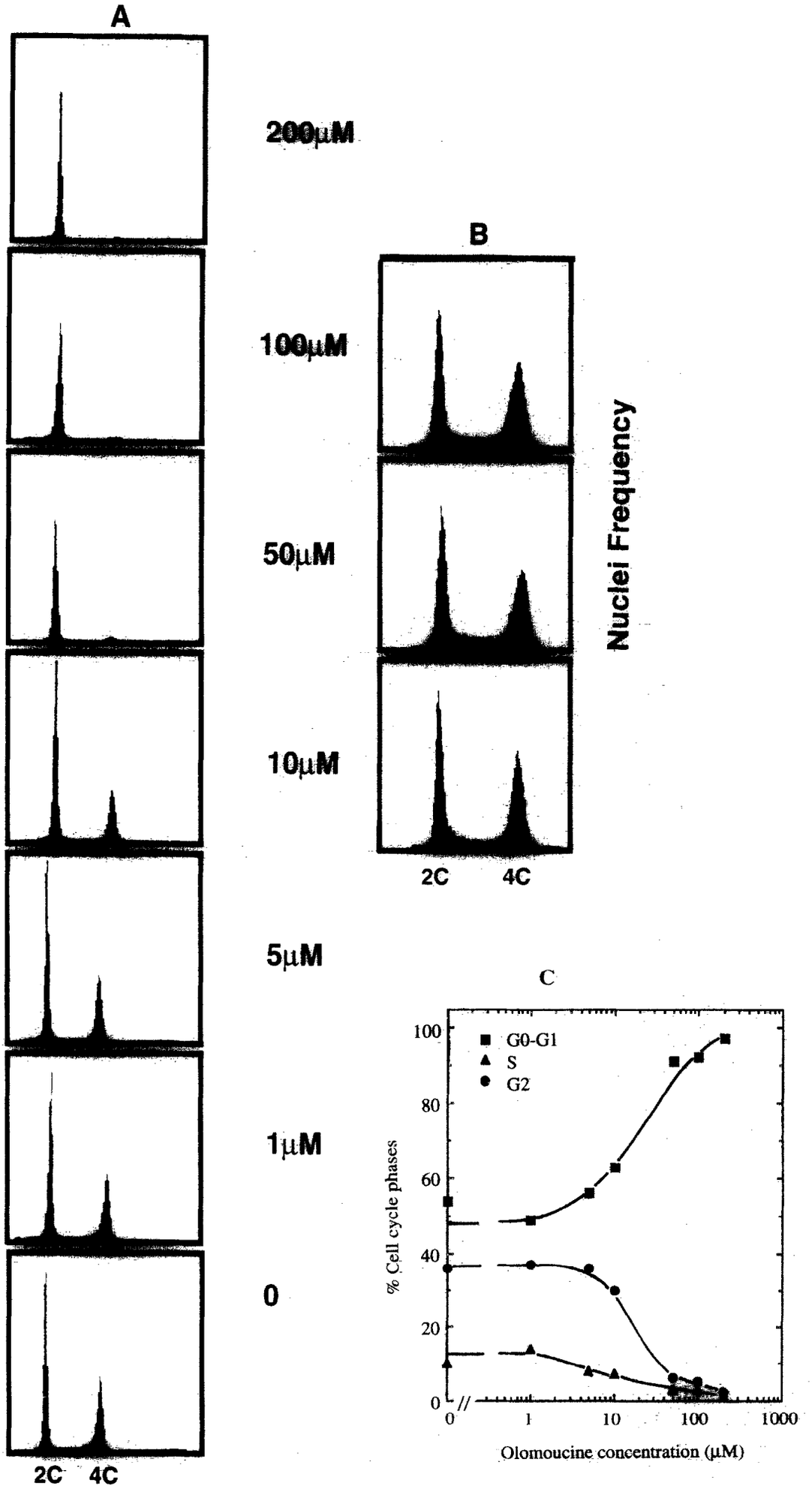

Fig 4. Olomoucine inhibits the G1/S transition of *Petunia* protoplasts. Protoplasts were synchronized, exposed to various olomoucine concentrations, and their cell cycle status was analyzed by flow cytometry (A). B. Cell cycle distribution after washing the olomoucine. C. Quantification of A.

The precipitate/drug mixture was incubated at 37°C for 10 min and phosphorylation was initiated by addition of 20 µl of kinase buffer containing histone and [γ-^{32}P]ATP as described [50].

Results

Dinoflagellate and diatom (unicellular algae)

Cultures of the dinoflagellate *Amphidinium carterae* and the diatom *Thalassiosira weissflogii* were partially synchronized by exposure to total darkness for 36 h. Olomoucine was added and cultures were exposed to light. Cells were sampled, fixed and stained and their cell cycle status was analyzed by flow cytometry. Control cells entered in S phase; an olomoucine concentration-dependent inhibition of the G1/S transition was observed (IC_{50}: 40 µM) (fig 1).

Fucus spiralis zygote development (Chromophyta, Fucophycea)

Olomoucine was applied to zygotes of the algae *Fucus spiralis* after fertilization for 30 h. Cells which polarised and divided were scored as 'germinated'. Olomoucine was found to inhibit cell division with an IC_{50} of 32 µM (fig 2). Polarisation occurred in half the zygotes without cell division. This inhibition was reversed by washing: zygotes were treated with 100 µM olomoucine for 26 h, washed and incubated in artificial sea water. They polarised and divided the next day.

Laminaria digitata gametophytes (Pheophyta)

The effects of olomoucine on the development of gametophytes after 50 days of culture are shown in figure 3. Control gametophytes rapidly developed into tufts of haplostichous

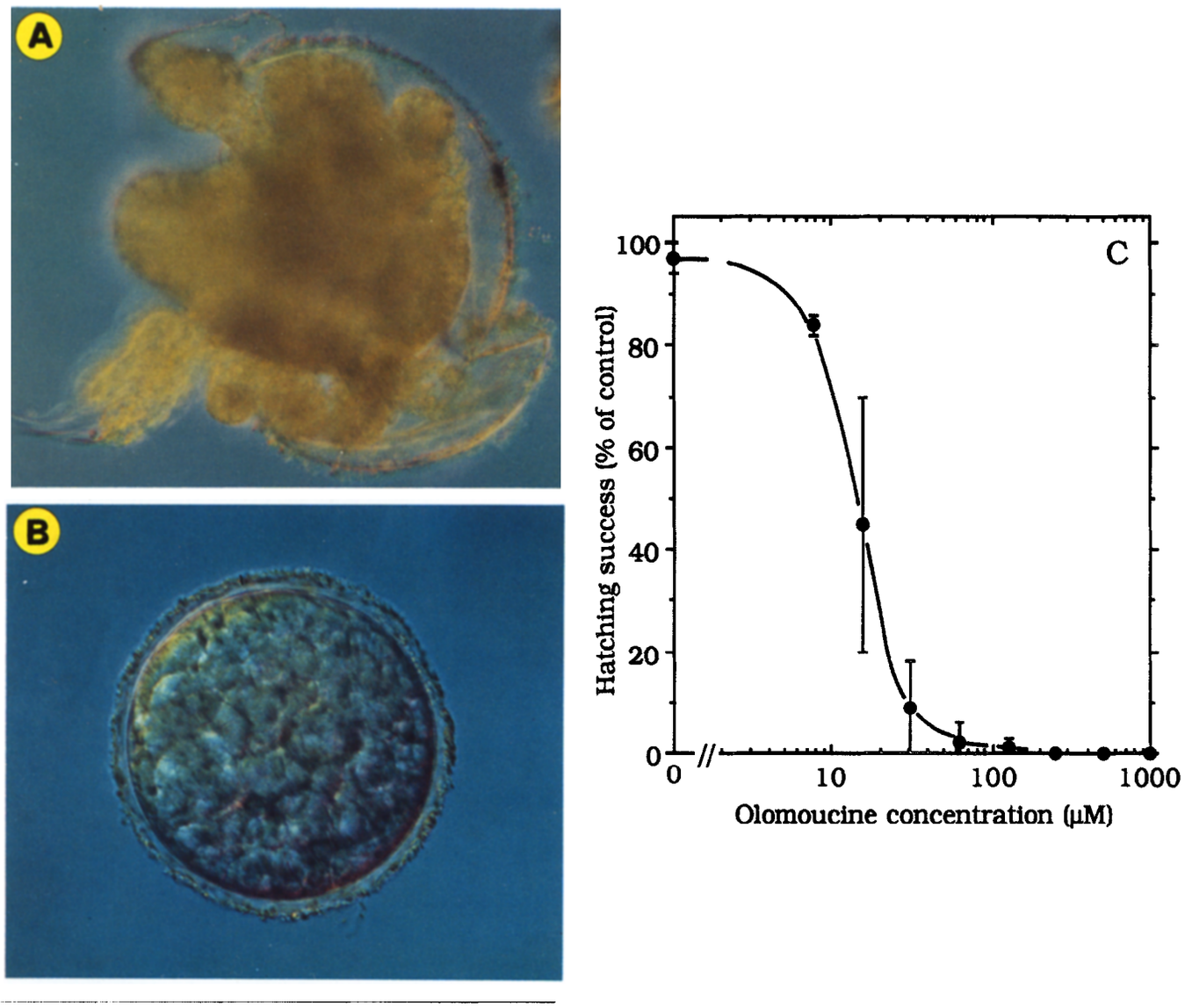

Fig 5. Olomoucine inhibits the development of *Calanus* embryos. **A.** Control nauplius after 30 h of development. **B.** Olomoucine (100 µM)-treated embryo after 30 h. **C.** Percent hatching as a function of olomoucine concentration.

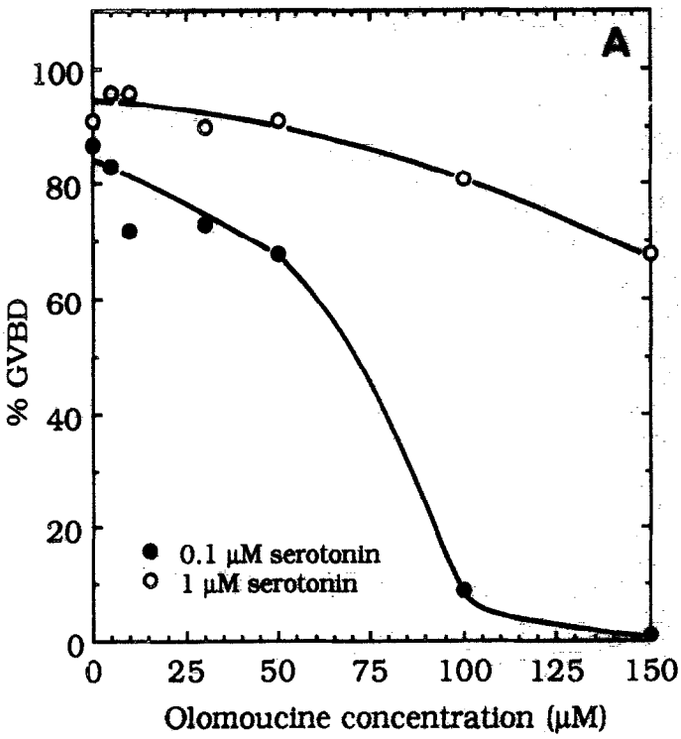

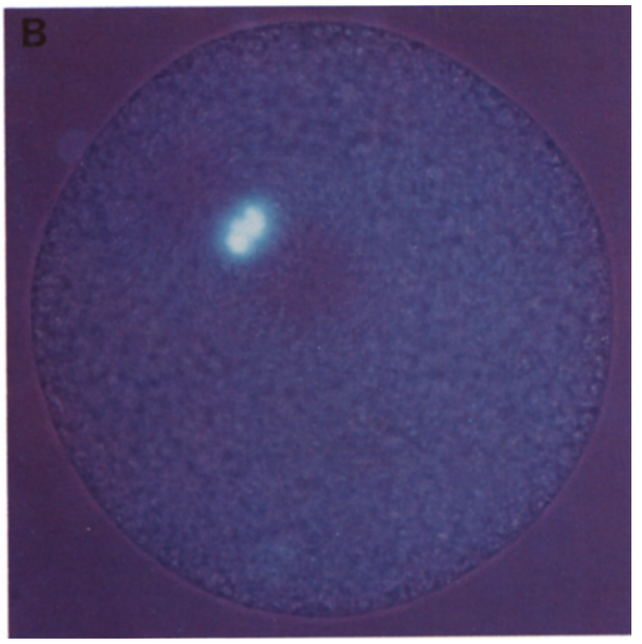

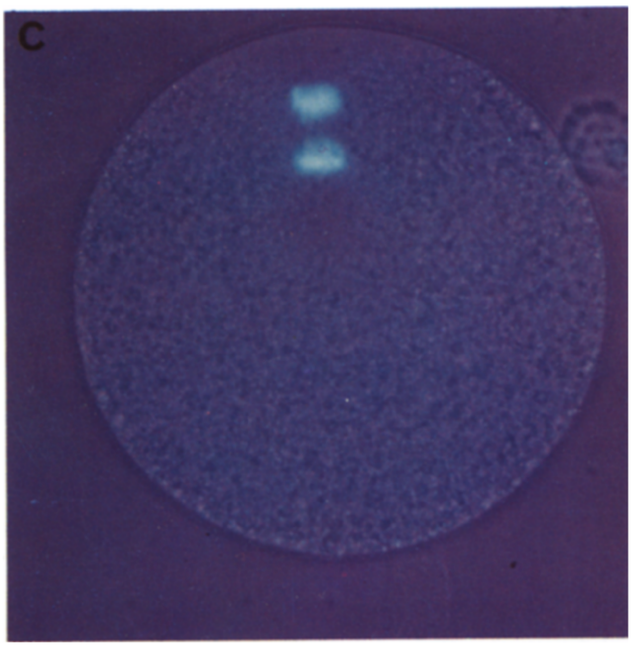

Fig 6. Olomoucine inhibits the prophase/metaphase transition of *Ruditapes* oocytes but triggers the release from metaphase I arrest. **A.** Prophase-arrested oocytes were exposed to various concentrations of olomoucine and treated with serotonin (0.1 and 1 μM). The percent germinal vesicle breakdown (GVBD) was scored. **B.** Control metaphase-arrested oocyte, following treatment with 0.1 μM serotonin, as observed under fluorescence after DNA staining; spindle and metaphase chromosomes are clearly distinguished. **C.** 15 min after addition of 120 μM olomoucine, the oocyte is activated and its chromosomes enter in anaphase.

filaments. About one-third of the gametophytes underwent gametogenesis, each fertile gametophyte bearing one or more polystichous sporophytes. Controls grown in the presence of DMSO also displayed normal growth, though they developed fewer and smaller, yet normally-shaped sporophytes. In the presence of 3–6 μM olomoucine gametophytes grew normally but very few, small and abnormally-shaped sporophytes were observed. At 12.5 μM olomoucine gametophytes had a reduced growth rate. Some of them did not develop beyond a few divisions. No sporophytes were observed. At 25 μM olomoucine gametophytes either did not elongate, enlarging 3–5-fold in size or only grew swollen, undivided filaments. At 50 μM olomoucine, gametophytes either did not germinate or developed into swollen roundish buds. The survival rate of gametophytes at 50 days was not significantly affected up to 100 μM olomoucine.

Petunia hybrida protoplasts (Phanerophyta)

Protoplasts were isolated from differentiated mesophyll cells and exposed, 14 h later, to various concentrations of olomoucine. The distribution of nuclei in the cell cycle

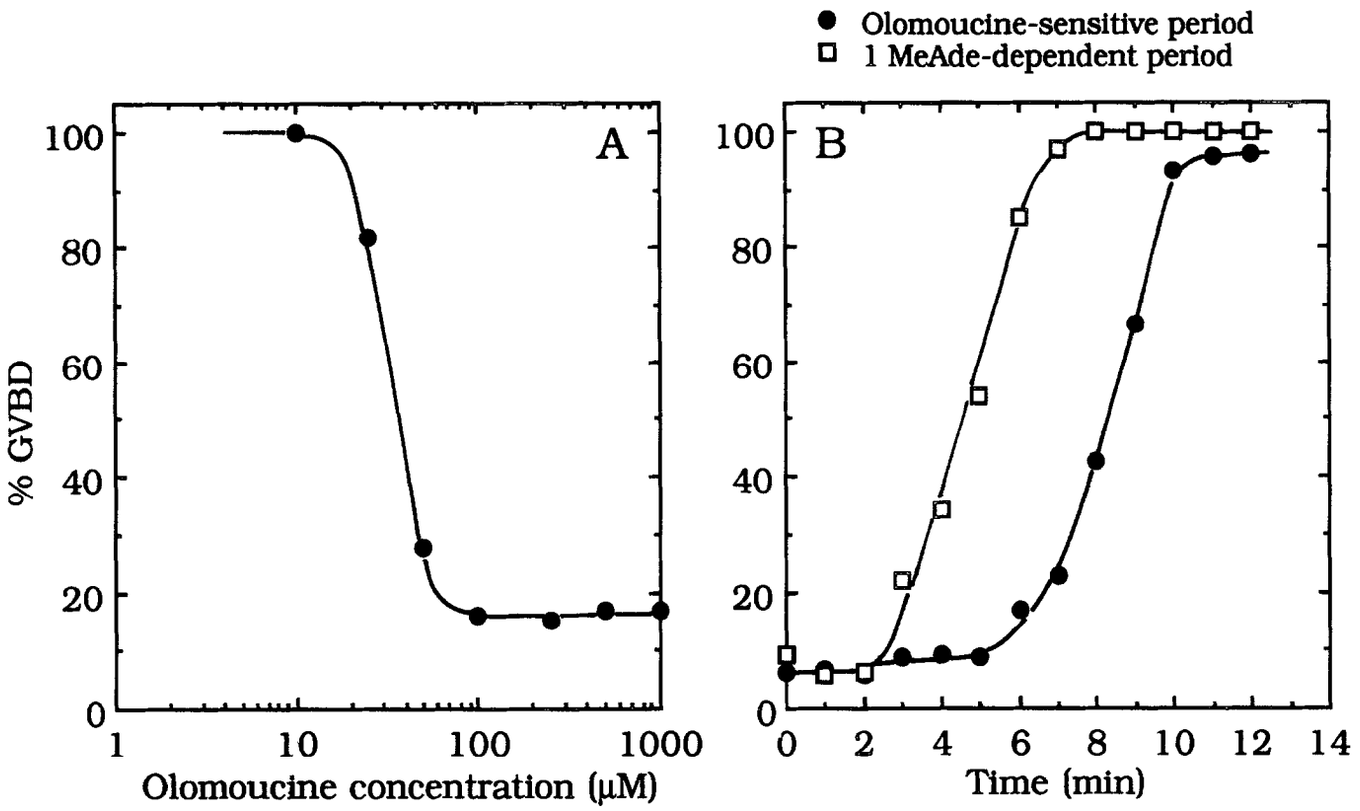

Fig 7. Olomoucine inhibits the maturation of starfish oocytes. **A.** Prophase-arrested oocytes were exposed to various concentrations of olomoucine and treated with 1 μM 8-hydroxyeicosatetraenoic acid. The percent GVBD was scored. **B.** The 1-methyladenine-dependent period was determined by diluting aliquots of a 1-methyladenine-stimulated oocyte population to non-efficient concentrations and scoring the percent GVBD after 30 min. The olomoucine-sensitive period was determined by stimulating an oocyte population with 1 μM 1-methyladenine and adding 100 μM olomoucine at various times to 1 ml aliquots of the oocyte suspension. The percent GVBD was scored after 30 min.

phases was investigated by flow cytometry. Increasing concentrations of olomoucine lead to an arrest in the G1 phase and a gradual decrease of the S and G2 populations (fig 4A, 4C). When olomoucine was eliminated by washing, the protoplasts were released from the G1 arrest and entered the S and G2 phases (fig 4B). G1 arrest caused by olomoucine was associated with an increase in cell size (data not shown). A G2 arrest was also observed [10].

Caenorhabditis elegans embryos (Nematoda)

Under normal conditions the timing and sequence of divisions in *C elegans* embryos is rigourously fixed [49, 50]. At concentrations up to 1 mM, olomoucine had no effect on *C elegans'* early development. Since this lack of effect might be due to the chemical barrier provided by the vitelline membrane [50], the egg envelope was fenestrated with a laser microbeam prior to exposure to olomoucine (table I). Below 100 μM olomoucine, no significant difference in timing, sequence or polarity of early cleavages (from the 2-cell to 24-cell stage) was observed. At 100 μM, a slight retardation of cleavage was observed. At 1 mM olomoucine a considerable retardation took place. Other parameters remained unaltered, except the size of nuclei which became enlarged. At 2 mM olomoucine, retardation was apparently stronger than at 1 mM; however, only a few divisions occurred. The retardation effect was apparently totally reversible since cleavage took place at essentially normal timing ($n = 3$) upon removal of olomoucine (2 mM) from the medium.

Table I. Timing of *Caenorhabditis elegans* early development (from AB to P4) in the presence of olomoucine.

Conditions	*Development time (AB to P4)(min-max)*	*n*	*normal timing (%)*
Control (no laser fenestration)	48 min (44-53)	4	100
Control (laser fenestration, + 1% DMSO)	47.5 min (46-49)	4	100
100 μM olomoucine	50.5 min (46-55)	11	106
1000 μM olomoucine	72.5 min (68-77) (+ 1 × 94)	4	153
2000 μM olomoucine	only early cleavages	3	*ca* 180

Calanus helgolandicus embryo development (Arthropoda, Crustacea)

Embryos of the copepod *Calanus helgolandicus* were cultivated in the presence of various olomoucine concentrations. After 30 h, control embryos had developed into free-swimming larvae, the nauplii (fig 5A). In contrast, olomoucine-treated embryos underwent a concentration-dependent inhibition of cell division, and hence, of development (fig 5B). These abnormal embryos displayed globular, cell-like struc-

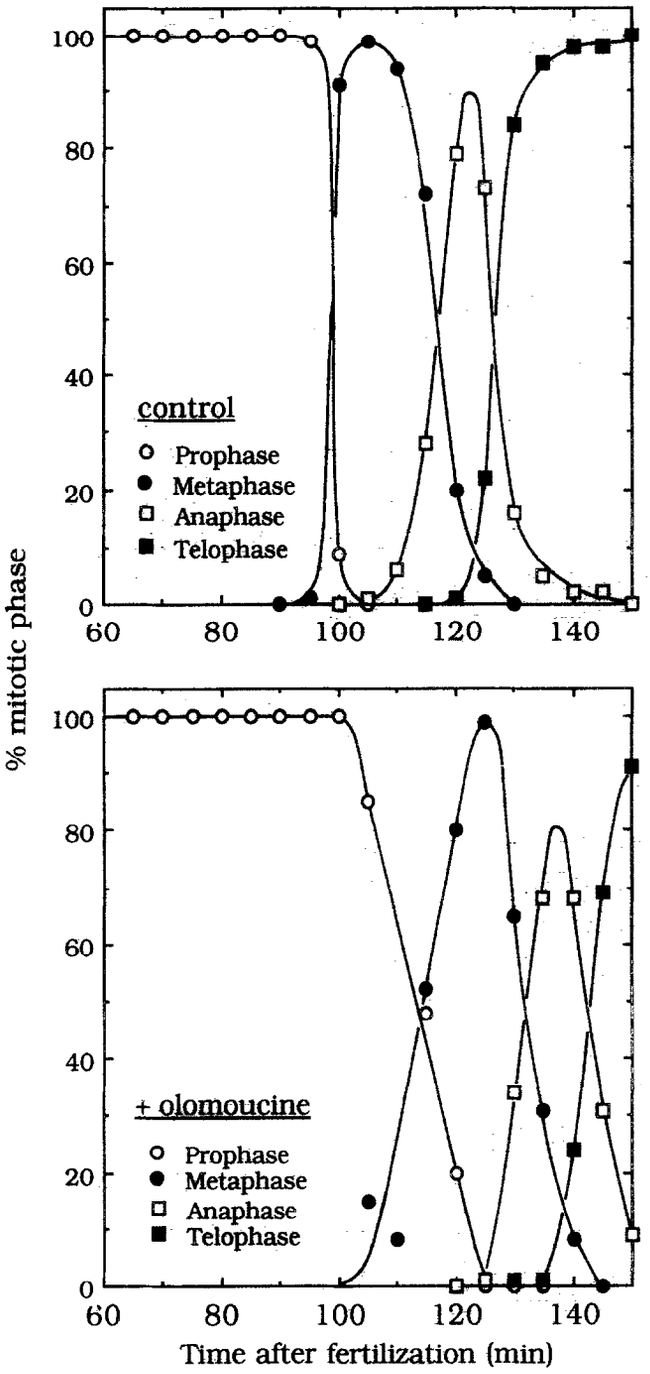

Fig 8. Olomoucine delays the prophase/metaphase transition of sea urchin embryos. Sea urchin eggs were fertilized and exposed to 100 μM olomoucine at 60 min post-fertilization. Aliquots of the egg suspension were taken at various times and processed for microscopic determination of their cell cycle phase. Top panel, control eggs. Lower panel, olomoucine-treated eggs.

tures with condensed chromatin, never hatched and ultimately died. A 50% inhibition of hatching occurred at 15 μM (fig 5C).

Oocyte maturation in Ruditapes philippinarum (Mollusca, Pelecypoda)

Upon stimulation by serotonin (5-hydroxytryptamine) prophase-arrested clam oocytes enter the first meiotic division up to metaphase I [1, 14]. This prophase/metaphase transition was reversibly inhibited by olomoucine (IC_{50}: 75 μM) (fig 6A). Metaphase I-arrested oocytes (fig 6B) were also exposed to olomoucine. This treatment released the oocytes from their arrest: they entered into anaphase (fig 6C), eventually released a polar body, and reformed nuclei (not shown).

Oocyte maturation in starfish (Echinodermata, Asteroidea)

Starfish oocytes are naturally arrested in the late prophase of the first meiotic division; the follicle cells-derived hormone 1-methyladenine triggers re-entry into meiosis (for review see [28]). In a previous paper [62] we showed that the prophase/metaphase transition of starfish oocytes, triggered by 1-methyladenine, is inhibited by olomoucine (IC_{50}: 30 μM). We have confirmed this inhibitory effect with two mimetics of the hormone, calyculin A, a protein phosphatase inhibitor (data not shown) and 8-hydroxyeicosatetraenoic acid [27] (fig 7A). In order to undergo maturation, the oocytes must be in contact with 1-methyladenine for a so-called 'hormone-dependent period' [30]. Clearly the oocytes remain sensitive to olomoucine beyond this hormone-dependent period (fig 7B).

Prophase/metaphase transition in sea urchin embryos (Echinodermata, Echinoidea)

Addition of 100 μM olomoucine to fertilized sea urchin eggs did not inhibit cleavage. However, we observed a consistent delay in the onset of cleavage. When further analyzed, this delay was found to be restricted to an increased duration of the prophase/metaphase transition (fig 8). The duration of the metaphase/anaphase and anaphase/telophase transitions was not significantly modified in olomoucine-treated embryos.

Ascidian eggs (Chordata, Ascidiacea)

Unfertilized *Phallusia mammillata* oocytes are naturally arrested in the first meiotic metaphase [11]. At a concentration of 100 μM, olomoucine failed to trigger the release from this arrest. Oocytes were then fertilized prior to exposure to olomoucine. Either no zygote cleavage or abnormal cleavages, eventually leading to some abnormal blastulae, were observed after 90 min of incubation (fig 9). In contrast, non-treated zygotes underwent synchronous cleavages leading to gastrulae, and finally to tadpole larvae.

Xenopus laevis oocytes (Amphibia)

Prophase-arrested *Xenopus* oocytes were simultaneously treated with progesterone and various concentrations of olomoucine. A dose-dependent inhibition of oocyte maturation was observed (fig 10A) (IC_{50}: 100 μM). Inhibition was slowly and partially reversed by washing and exposure to progesterone. The effect of olomoucine on the *in vivo* activity of the cdc2 kinase was estimated on the phosphorylation of the elongation factor subunits. This cdc2 substrate is phosphorylated on its γ subunit (threonine 230) [36] and on its δ subunit (threonine 122 and an unidentified serine) [37]. The whole elongation factor 1 complex was immunoprecipitated from ^{32}P-labelled oocytes (prophase-arrested, progesterone-treated, progesterone- and olomoucine-treated), resolved by SDS-PAGE and autoradiography. Olomoucine inhibited the phosphorylation of EF-1 γ and δ (fig 10B). Finally, *in vitro* phosphorylation of elongation factor 1 by purified cdc2 kinase was measured in the presence of various concentrations of olomoucine and 50 μM [^{32}P]-ATP. A dose-dependent inhibition was observed with an IC_{50} below 30 μM (fig 10C).

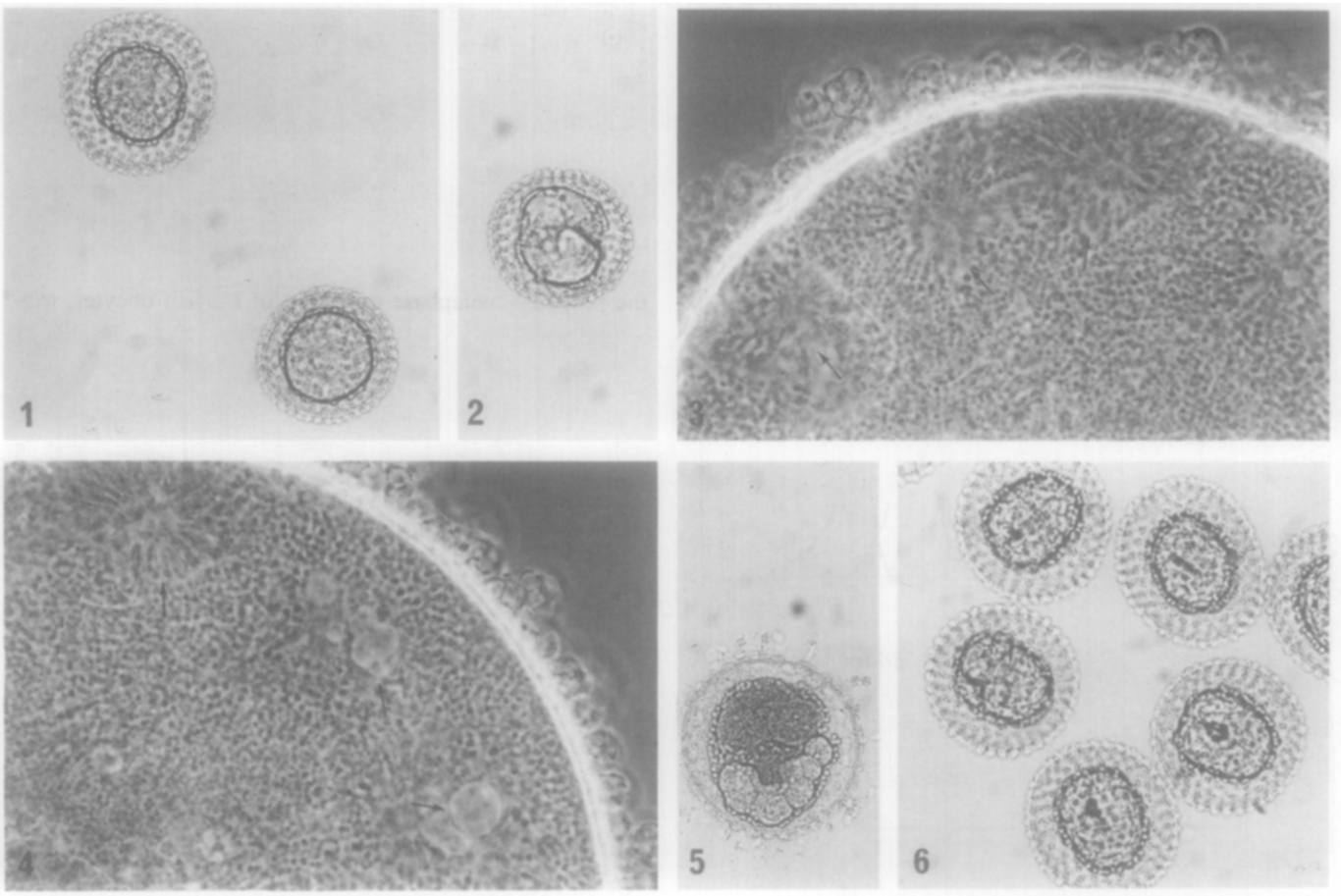

Fig 9. Olomoucine inhibits cleavage of Ascidian embryos. Oocytes were fertilized prior to exposure to 100 μM olomoucine. Undivided **(1)** or abnormally cleaved **(2)** embryos 5 h after fertilization, containing several mitotic spindles and nuclei **(3, 4); 5.** Abnormal blastulae; **6.** Control embryos have reached the 8-cell stage 90 min after fertilization.

Mouse oocytes

Mouse oocytes are released from their meiotic prophase arrest upon incubation in culture media. This process, scored by the time-course of germinal vesicle breakdown, was delayed in the presence of olomoucine (fig 11A). Spontaneously matured oocytes arrest in metaphase II, from which they can be released by fertilization or by parthenogenetic activation. This metaphase/interphase transition, measured by the formation of pronuclei, was accelerated by olomoucine (fig 11B).

Rhadomyosarcomas cell lines

Childhood rhabdomyosarcomas cells were grown in the presence of increasing concentrations of olomoucine. Growth inhibition was observed in the presence of olomoucine with IC_{50}s ranging from 18.4 to 85.7 μM (fig 12).

MCF-7 / MCF-7mdr and KB-3-1 / KB-A cell lines

Olomoucine has been tested on two cell lines, MCF-7 and KB-3-1 and their adriamycin-resistant sublines, MCF-7mdr and KB-A. After 24 h and 48 h of culture in the presence of olomoucine, [^{3}H]thymidine incorporation was estimated by a 30 min pulse. [^{3}H]-Thymidine incorporation was inhibited in a dose-dependent manner. IC_{50}s (approximatively 25 μM) were quite similar for normal and adriamycin-resistant cell lines (fig 13).

NCI disease-oriented in vitro screen

Olomoucine (0.01–100 μM; 48 h exposure) has been tested on 60 human tumor cell lines comprising nine tumor types (leukemia, non-small cell lung cancer, colon cancer, central nervous system cancer, melanoma, ovarian cancer, renal cancer, prostate cancer, breast cancer). All cell lines displayed a similar sensitivity to olomoucine (data not shown). The average IC_{50} was 60.3 μM.

Non-small cell lung cancer cell line MR65

The non-small cell lung cancer cell line MR65 was grown, pulse-labeled with BrdU and treated with various concentrations of olomoucine. After various periods of time cultures were harvested and cell cycle parameters were analyzed as described in the *Materials and methods* section. Results show that olomoucine does not produce obvious differences in cell cycle distribution, nor in the G2/M exit rate for the cells that were originally in G2/M (G2M-) at the time of BrdU labeling. However a dose-dependent decrease in G1 phase entry rate (F+), in S phase entry rate (G1S), in S phase transit time (relative moment) and in G1 phase exit rate (G1–) was observed (fig 14).

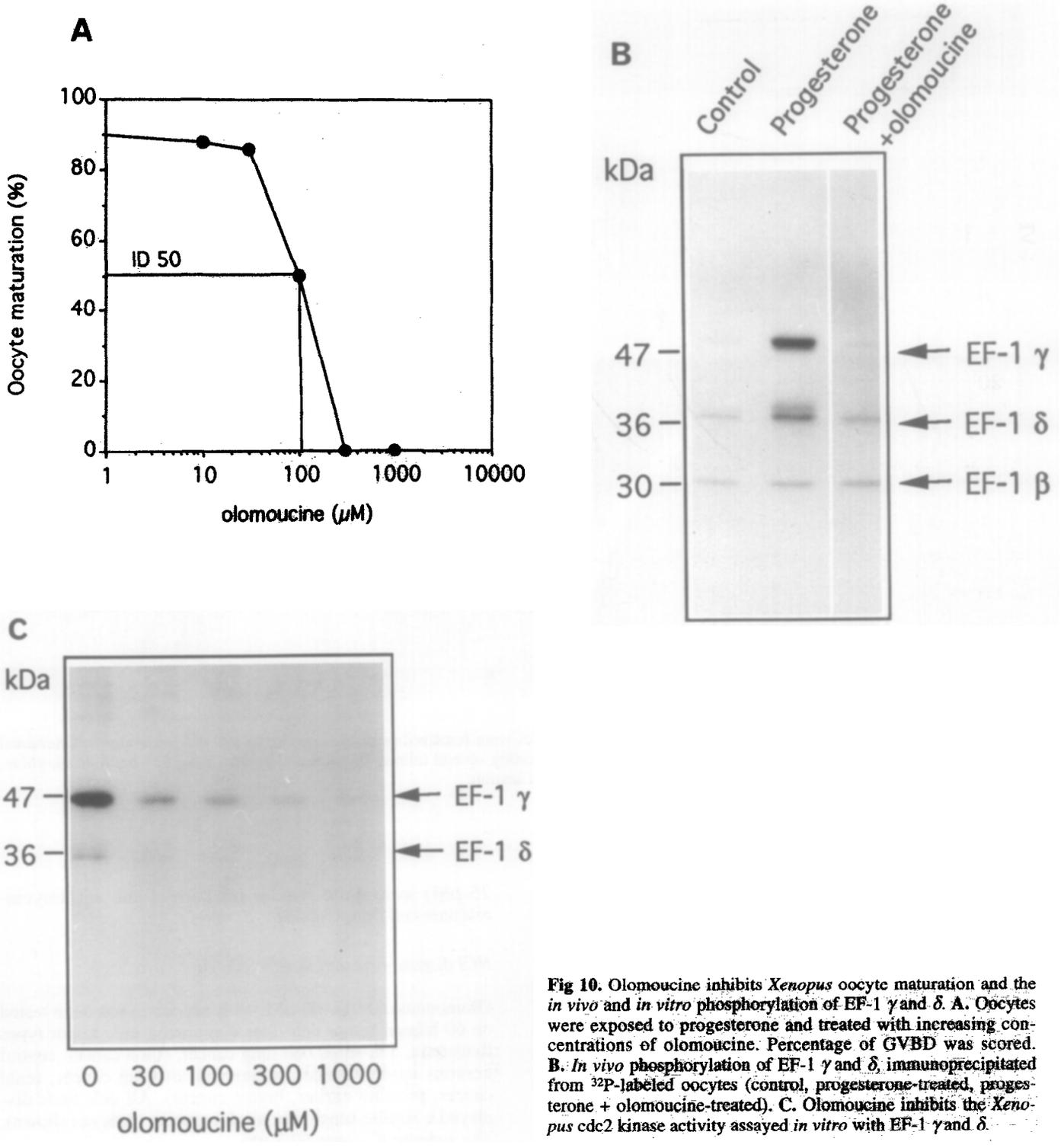

Fig 10. Olomoucine inhibits *Xenopus* oocyte maturation and the *in vivo* and *in vitro* phosphorylation of EF-1 γ and δ. **A.** Oocytes were exposed to progesterone and treated with increasing concentrations of olomoucine. Percentage of GVBD was scored. **B.** *In vivo* phosphorylation of EF-1 γ and δ, immunoprecipitated from ^{32}P-labeled oocytes (control, progesterone-treated, progesterone + olomoucine-treated). **C.** Olomoucine inhibits the *Xenopus* cdc2 kinase activity assayed *in vitro* with EF-1 γ and δ.

Interleukin-2-stimulated T lymphocytes

CTLL-2 cells were treated with various concentrations of olomoucine. [^{3}H]thymidine incorporation in CTLL-2 cells was evaluated following interleukin-2 stimulation. A clear dose-dependent inhibition was observed (fig 15A). The effect of olomoucine on cell cycle distribution was further tested by FACS analysis of cells under various conditions (table II). The distribution of log-growth cells was not altered by a 100 μM olomoucine treatment. A small reduction of S phase cells and a slight increase of G2 phase cells were observed, probably due to the exit of a fraction of these cells from the S phase and their subsequent arrest in G2. Cells were next synchronized in late G1, by IL-2 deprivation for 12 h. Cells were then restimulated by IL-2 in the absence or presence of olomoucine. IL-2 deprivation triggered a marked G1 arrest (table II) from which cells were released upon IL-2 restimulation. Cells remained arrested in G1 in the presence of olomoucine (table II). Finally, olomoucine was

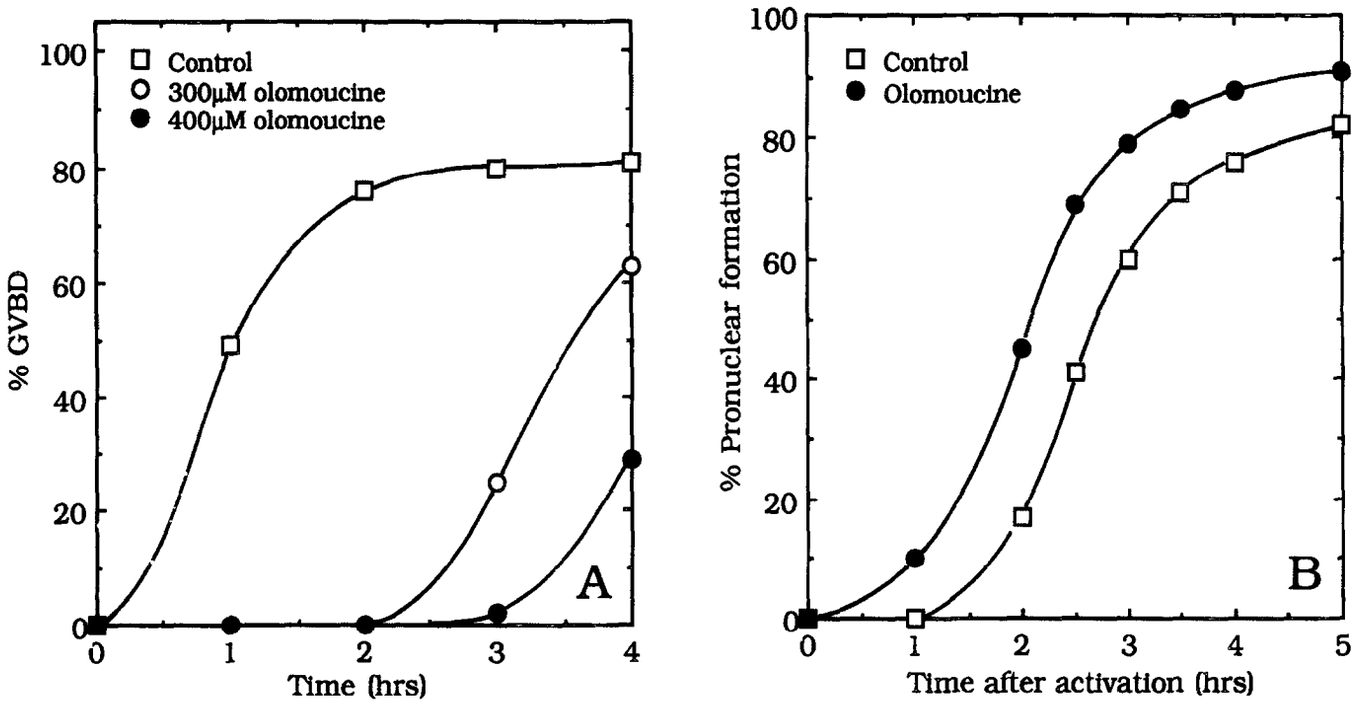

Fig 11. Olomoucine inhibits mouse oocyte maturation but facilitates their release from metaphase II arrest. **A.** The percent GVBD of spontaneously maturing oocytes, treated or not with olomoucine, was recorded. **B.** Metaphase II-arrested were parthenogenetically activated in the absence or presence of 100 μM olomoucine and the time-course of pronucleus formation was scored.

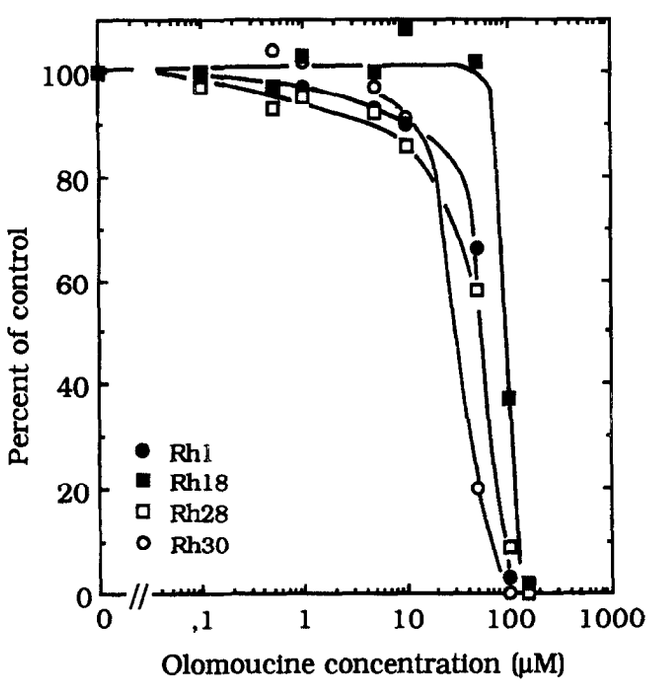

Fig 12. Olomoucine inhibits growth of rhabdomyosarcoma cell lines. Cells were cultivated in the presence of various olomoucine concentrations and their growth was recorded after 7 days.

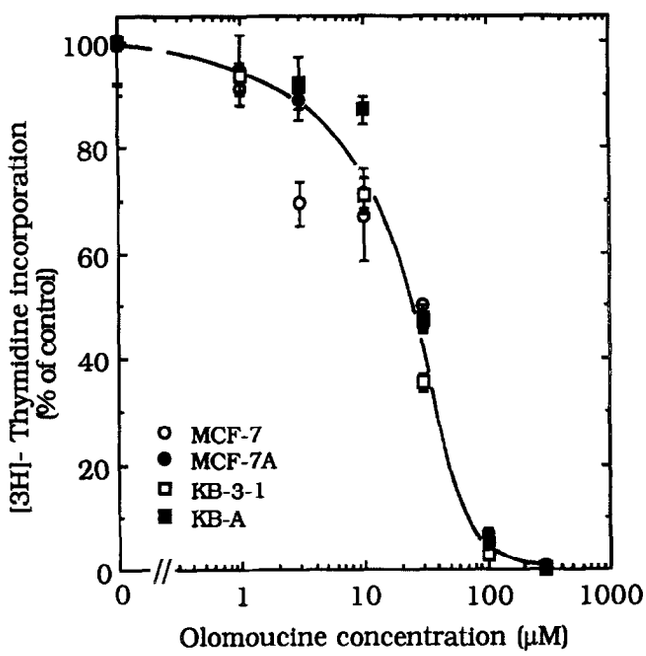

Fig 13. Olomoucine inhibits [^{3}H]-thymidine incorporation of MCF-7 and KB-3-1 cells as well as of their adriamycin-resistant counterparts. Cells were grown in the presence of various concentrations of olomoucine, pulse-labeled with [^{3}H]-thymidine and processed for determination of incorporation in DNA.

tested against the cdc2 and cdk2 kinases respectively prepared from nocodazole- and hydroxyurea-treated CTLL-2 cells (fig 15B). IC_{50}s were 40 μM and 20 μM, respectively.

Discussion

Among 35 kinases tested, cdc2, cdk2, cdk5 (IC_{50}s: 3–10 μM) and the MAP kinase erk1 (IC_{50}: 25 μM) were found to

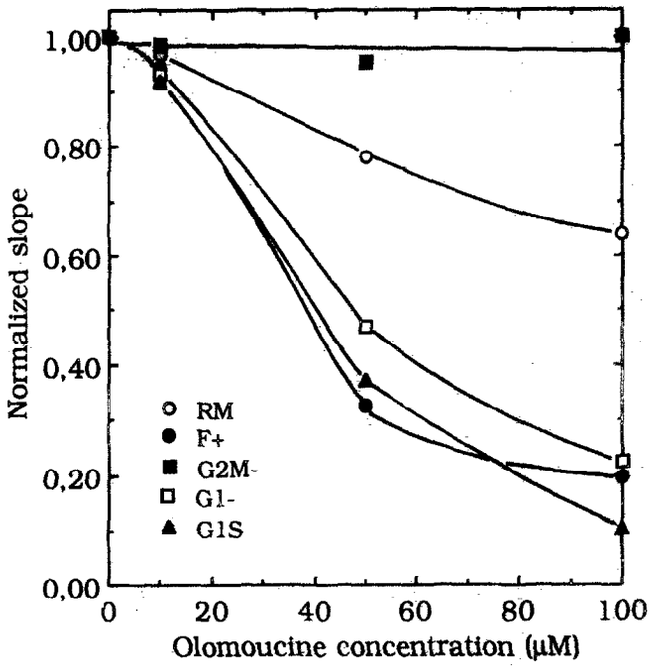

Fig 14. Olomoucine inhibits the cell cycle of non-small cell lung cancer cell line MR65. The non-small cell lung cancer cell line MR65 was grown, pulse-labeled with BrdU and treated with various concentrations of olomoucine. After various periods of time cultures were harvested and cell cycle parameters were analyzed as described in *Materials and methods*. RM (relative moment), S phase transit time. F+, G1 phase entry rate. G2M-, G2/M exit rate for the cells that were originally in G2/M at the time of BrdU labeling. G1-, G1 phase exit rate. G1S, S phase entry rate.

Table II. Cell cycle distribution of CTTL-2 cells cultivated under various conditions.

Sample	*G1 (%)*	*S (%)*	*G2/M (%)*
Log-growth	42	36	21
+ olomoucine (100 μM)	48	19	32
G1 arrest	76	7	16
G1 arrest + restimulation at 16 h	42	48	9
G1 arrest + restimulation at 16 h + olomoucine (100 μM)	77	7	15

be inhibited by olomoucine, a C^2,N^6,N^9-substituted purine [62]. Olomoucine acts as a competitive inhibitor for ATP binding as shown by a classical enzymological approach [62] and, more directly, by structural analysis of a cdk2/olomoucine co-crystal [51]. Interestingly the purine of olomoucine and the purine of ATP are orientated in a totally different manner, and this may be the basis for the unique selectivity of olomoucine, despite its competitive action at the ATP binding site. The unusual selectivity of olomoucine prompted us to investigate its effects on a variety of cell cycle models.

There are a few examples where little or no effects were observed: yeast (P Nurse, personal communication), *Drosophila* embryos (B Edgar, personal communication). Similarly cleavage of nematode (*C elegans*) embryos was only

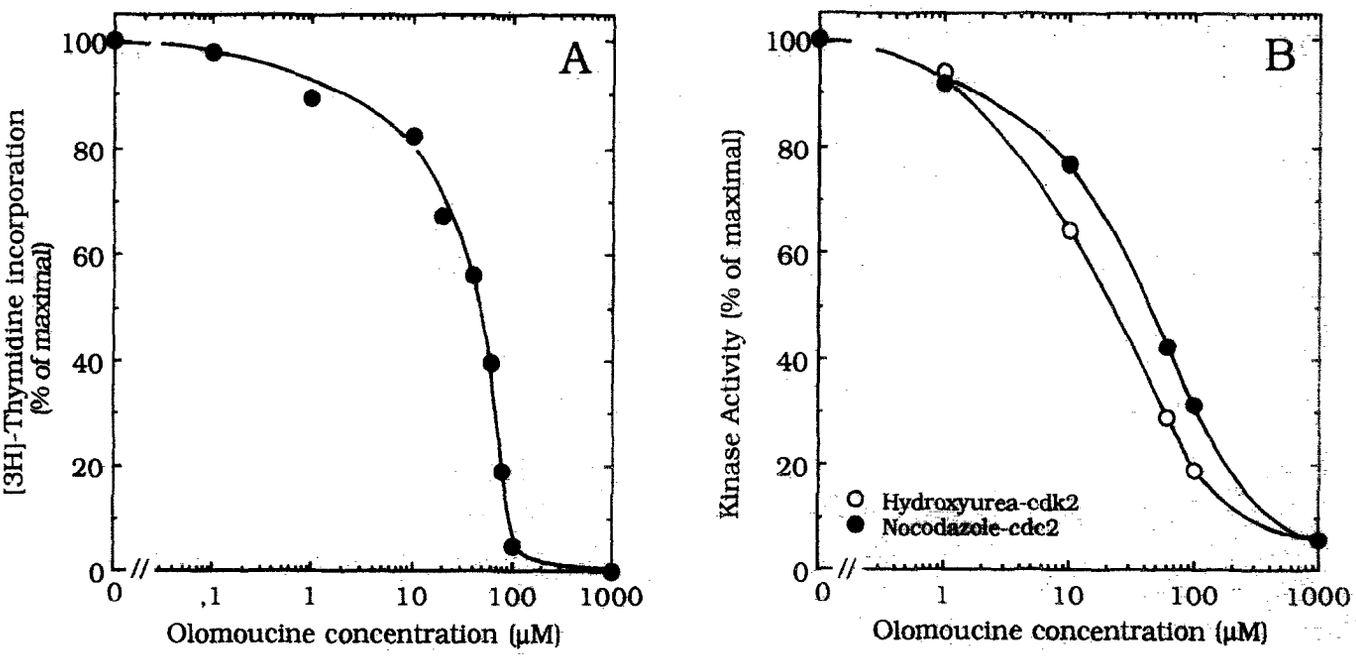

Fig 15. Olomoucine inhibits the cell cycle of interleukin-2-stimulated T lymphocytes (CTTL-2) (**A**) and their cdc2 and cdk2 kinases (**B**). **A.** Cells were treated with interleukin-2, grown in the presence of various concentrations of olomoucine, pulse-labeled with [^{3}H]-thymidine and processed for determination of incorporation in DNA. **B.** Histone H1 kinase activity was assayed in anti-cdk2 and anti-cdc2 immunoprecipitates prepared from hydroxyurea- and nocodazole-treated CTTL-2 cells, respectively, in the presence of increasing concentrations of olomoucine.

sensitive to very high concentrations of olomoucine. This lack of effect can be tentatively ascribed to poor permeability of the plasma membrane of these cells to the drug, rapid inactivating mechanisms, extrusion of the drug or fast compartmentalisation away from the potential targets.

In several examples we have observed a general inhibition of proliferation without further analyzing the stage of cell cycle inhibition: development of algae embryos and gametophytes (*Fucus, Laminaria*), copepods and ascidian embryos, several human cell lines (rhabdomyosarcoma cell lines, NCIs 60 human tumor cell lines, MCF-7, KB-3-1).

Natural or artificial synchrony in the other models has allowed us to analyze the cell cycle stage specificity of olomoucine action.

A G1 arrest was observed in unicellular algae (dinoflagellate, diatom), *Petunia* protoplasts, non-small cell lung cancer cell line MR65, interleukin-2-stimulated T lymphocytes. This G1 arrest is consistent with an inhibition of cdk2 in olomoucine-treated cells. A large body of evidence demonstrates the essential role of cdk2, associated with cyclins E and A, in the regulation of the G1/S transition (for review see [59]). To illustrate with a genetic example, a dominant-negative mutation of cdk2 arrests human U2OS cells in G1 [59].

A prophase arrest ('G2 arrest') was observed in clam, starfish, *Xenopus* oocytes, while the prophase/metaphase transition was slowed down in sea urchin embryos and mouse oocytes. This effect is consistent with an effect of olomoucine on cdc2/cyclin B, the universal M phase-promoting factor. Here also a wealth of data demonstrate the complete dependence of this cell cycle phase transition on active cdc2 kinase (for review see [59]). To illustrate with a genetic evidence, a mouse cell line (FT 210) carrying a temperature-sensitive mutation on cdc2, arrests only in G2 at the restrictive temperature [58]. Dominant-negative cdc2 mutants arrest human U2OS cells at the G2/M transition [59].

Finally, in three examples (clam oocytes, sea urchin and mouse embryos), olomoucine was found to facilitate or even trigger the metaphase/anaphase transition. This effect is consistent with the inhibitory effect of active cdc2 kinase on the exit from mitosis [9, 24, 38].

Taken together these data show that olomoucine arrests cells both at the G1/S and the G2/M boundaries, consistent with the hypothesis of a prevalent effect on cdk2 and cdc2, respectively. We cannot exclude however an effect of olomoucine on MAP kinase, specially in growth-factors-stimulated cells. By its high selectivity, olomoucine provides an anti-mitotic reagent which preferentially inhibits certain steps of the cell cycle and may constitute a lead compound for the design of new anti-tumor agents.

Acknowledgment

This research was supported by a grant from the 'Association pour la Recherche sur le Cancer' (ARC 6268) (to LM) and the 'Fédération Nationale des Groupements des Entreprises Françaises et Monégasques dans la Lutte contre le Cancer' (FEGEFLUC) to LM.

References

1 Abdelmajid H, Colas P, Durocher Y, Gobet I, Guerrier P, Krantic S, Leclerc-David C, Moreau M, Néant I, Rivaillier P, Tomkowiak M (1993) Role of calcium during release of mollusc oocytes from their blocks in meiotic prophase and metaphase. *Biol Cell* 78, 137–143

2 Begg AC, McNally NJ, Shrieve DC, Karcher H (1985) A method to measure the duration of DNA synthesis and the potential doubling time from a single sample. *Cytometry* 6, 620–626

3 Bergounioux C, Perennes C (1980) Transfert de facteurs cytoplasmiques de la fertilité mâle entre deux lignées de *Petunia hybrida* par fusion de protoplastes. *Plant Sci Lett* 19, 143–149

4 Cowan KH, Batist G, Tulpule A, Sinha BK, Myuers CE (1986) Similar biochemical changes associated with multidrug resistance in human breast cancer cells and carcinogen-induced resistance to xenobiotics in rats. *Proc Natl Acad Sci USA* 83, 9328–9332

5 Dilling MB, Dias P, Shapiro DN, Germain GS, Johnson RK, Houghton PJ (1994) Rapamycin selectively inhibits the growth of childhood rhabdomyosarcoma cells through inhibition of signaling via the type I insulin-like growth factor receptor. *Cancer Res* 54, 903–907

6 Douglass EC, Valentine M, Etcubanas E, Parham DM, Webber BL, Houghton PJ, Green AA (1987) A specific chromosomal abnormality in rhabdomyosarcoma. *Cytogenet Cell Genet* 45, 148–155

7 El-Deiry WS, Tokino T, Velculescu VE, Levy DB, Parsons R, Trent JM, Lin D, Mercer E, Kinzler KW, Vogelstein B (1993) WAF1, a potential mediator of p53 tumor suppression. *Cell* 75, 817–825

8 Galbraith DW, Harkins KR, Maddox JM, Ayres NM, Sharma DP, Firoozabady E (1983) Rapid flow cytometric analysis of the cell cycle in intact plant tissues. *Science* 220, 1049–1051

9 Gallant P, Nigg EA (1992) Cyclin B2 undergoes cell cycle-dependent nuclear transport and, when expressed as a non destructable mutant, causes mitotic arrest in HeLa cells. *J Cell Biol* 117, 213–224

10 Glab N, Labidi H, Qin L-X, Trehin C, Bergounioux C, Meijer L (1994) Olomoucine, an inhibitor of the cdc2/cdk2 kinases, blocks plant cells at the G1 to S and G2 to M cell cycle transitions. *FEBS Lett* 353, 207–214

11 Goudeau H, Goudeau M, Guibourt N (1992) The fertilization potential and associated membrane potential oscillations during the resumption of meiosis in the egg of the ascidian *Phallusia mammillata*. *Dev Biol* 153, 227–241

12 Grever MR, Schepartz SA, Chabner BA (1992) The National Cancer Institute: Cancer Drug Discovery and Development Program. *Sem Oncol* 19, 622–638

13 Gu Y, Turck CW, Morgan DO (1993) Inhibition of cdk2 activity *in vivo* by an associated 2OK regulatory subunit. *Nature* 366, 707–710.

14 Guerrier P, Leclerc-David C, Moreau M (1993) Evidence for the involvement of internal Ca^{2+} stores during serotonin-induced meiosis reinitiation in oocytes of the bivalve *Ruditapes philippinarum*. *Dev Biol* 159, 474–484

15 Harper JW, Adami GR, Wei N, Keyomarsi K, Elledge SJ (1993) The p21 cdk-interacting protein Cip1 is a potent inhibitor of G1 cyclin-dependent kinases. *Cell* 75, 805–816

16 Hazelton BJ, Houghton JA, Parham DM, Douglass EC, Torrance PM, Holt H, Houghton PJ (1987) Characterization of cell lines derived from xenografts of childhood rhabdomyosarcoma. *Cancer Res* 47, 4501–4507

17 Hidaka H, Kobayashi R (1992) Pharmacology of protein kinase inhibitors. *Annu Rev Pharmacol Toxicol* 32, 377–397.

18 Higashikubo R, White RA, Roti JL (1993) Flow cytometric BrdUrd-pulse-chase study of heat-induced cell-cycle progression delays. *Cell Prolif* 26, 337–348

19 Kamb A, Gruis NA, Weaver-Feldhaus J, Liu Q, Harshman K, Tavtigian SV, Stockert E, Day III RS, Johnson BE, Skolnick MH (1994) A cell cycle regulator potentially involved in genesis of many tumor types. *Science* 264, 436–440

20 Keller MD, Selvin RC, Claus W, Guillard RRL (1987) Media for the culture of oceanic ultraphytoplancton. *J Phycol* 23, 633–638

21 Kitagawa M, Okabe T, Ogino H, Matsumoto H, Suzuki-Tak-

ahashi I, Kokubo T, Higashi H, Saitoh S, Taya Y, Yasuda H, Ohba Y, Nishimura S, Tanaka N, Okuyama A (1993) Butyrolactone I, a selective inhibitor of cdk2 and cdc2 kinase. *Oncogene* 8, 2425–2432

22 Kropf DL (1992) Establishment and expression of cellular polarity in fucoid zygotes. *Microbiol Rev* 56, 316–339

23 Kubiak JC, Weber M, de Pennart H, Winston N, Maro B (1993)The metaphase II arrest in mouse oocytes is controlled through microtubule-dependent destruction of cyclin B in the presence of CSF. *EMBO J* 12, 3773–3781

24 Luca FC, Shibuya EK, Dohrmann CE, Ruderman JV (1991) Both cyclin AΔ60 and BΔ97 are stable and arrest cells in M phase, but only cyclin BΔ97 turns on cyclin destruction. *EMBO J* 10, 4311–4320

25 Maro B, Kubiak J, Verlhac MH, Winston NJ (1994) Interplay between the cell cycle control machinery and the microtubule network in mouse oocytes. *Sem Dev Biol* 5, 191–198

26 Meijer L (1995) Chemical inhibitors of cyclin-dependent kinases. *In: Progress in Cell Cycle Research* (Meijer L, Guidet S, Tung HYL, eds), Plenum Press New York, in press

27 Meijer L, Brash AR, Bryant RW, Ng K, Maclouf J, Sprecher H (1986) Stereospecific induction of starfish oocyte maturation by 8(R)-hydroxy-eicosa-tetraenoic acid [8(R) HETE]. *J Biol Chem* 261, 17040–17047

28 Meijer L, Mordret G (1994) Starfish oocyte maturation: from prophase to metaphase. *Sem Dev Biol* 5, 165–171

29 Meijer L, Pondaven P (1988) Cyclic activation of histone H1 kinase during the sea urchin egg mitotic divisions. *Exp Cell Res* 174 , 116–129

30 Meijer L, Pondaven P, Guerrier P, Moreau M (1986) A starfish oocyte user's guide. *Cah Biol Mar* 25, 457–480

31 Meyerson M, Enders GH, Wu CL, Su LK, Gorka C, Nelson C, Harlow E, Tsai LH (1992) A family of cdc2-related protein kinases. *EMBO J* 11, 2909–2917

32 Meyerson M, Harlow E (1994) Identification of G1 kinase activity for cdk6, a novel cyclin D partner. *Mol Cellul Biol* 14, 2077–2086

33 Morice WG, Brunn GJ, Wiederrecht G, Siekierka JJ, Abraham RT (1993) Rapamycin-induced inhibition of $p34^{cdc2}$ kinase activation is associated with G1/S-phase growth arrest in T lymphocytes. *J Biol Chem* 268, 3734–3738

34 Morice WG, Wiederrecht G, Brunn GJ, Siekierka JJ, Abraham RT (1993) Rapamycin inhibition of interleukin-2 dependent $p33^{cdk2}$ and $p34^{cdc2}$ kinase activation in T lymphocytes. *J Biol Chem* 268, 22737–22745

35 Motokura T, Arnold A (1993) Cyclins and oncogenesis. *Biochim Biophys Acta* 1155, 63–78

36 Mulner-Lorillon O, Cormier P, Cavadore J-C, Morales J, Poulhe R, Bellé R (1992) Phosphorylation of *Xenopus* elongation factor-1 gamma by cdc2 protein kinase: identification of the phosphorylation site. *Exp Cell Res* 202, 549–551

37 Mulner-Lorillon O, Minella O, Cormier P, Capony J-C, Cavadore J-C, Morales J, Poulhe R, Bellé R (1994) Elongation factor EF-1δ, a new target for MPF in *Xenopus* oocytes. *J Biol Chem* 269, 20201–20207

38 Murray AW, Solomon MJ, Kirschner MW (1989) The role of cyclin synthesis and degradation in the control of maturation promoting factor activity. *Nature* 339, 280–286

39 Néant I, Guerrier P (1988) 6-Dimethylaminopurine blocks starfish oocyte maturation by inhibiting a relevant protein kinase activity. *Exp Cell Res* 176, 68–79

40 Nigg EA (1993) Cellular substrates of p34cdc2 and its companion cyclin-dependent kinases. *Trends Cell Biol* 3, 296–301

41 Nobori T, Miura K, Wu DJ, Lois A, Takabayashi K, Carson DA (1994) Deletion of the cyclin-dependent kinase-4 inhibitor gene in multiple human cancers. *Nature* 368, 753-756

42 Noda A, Ning, Y, Venable SF, Pereira-Smith OM, Smith JR (1994) Cloning of senescent cell-derived inhibitors of DNA synthesis using an expression screen. *Exp Cell Res* 211, 90–98

43 Olson RJ, Zettler ER, Altabet MA, Dusenberry JA, Chisholm SW (1990) Spatial and temporal distribution of prochlorophyte picoplankton in the North Atlantic Ocean. *Deep-Sea Res* 37, 1033–1051

44 Otto FJ (1992) Preparation and staining of cells for high-resolution DNA analysis. *In: Flow Cytometry and Cell Sorting* (Radbruch A, ed) Springer-Verlag, Berlin

45 Perennes C, Qin L-X, Glab N, Bergounioux C (1993) Petunia $p34^{cdc2}$ protein kinase activity in G2/M cells obtained with a reversible cell cycle inhibitor, mimosine. *FEBS Lett* 333, 141–145.

46 Poulet SA, Ianora A, Miralto A, Meijer L (1994) Do diatoms arrest embryonic development in copepods ? *Mar Ecol Prog Series* 11, 79–86

47 Rialet V, Meijer L (1991) A new screening test for antimitotic compounds using the universal M phase-specific protein kinase, $p34^{cdc2}$/cyclin B^{cdc13}, affinity-immobilized on $p13^{suc1}$-coated microtitration plates. *Anticancer Res* 11, 1581–1590

48 Roninson IB, Chin JE, Choi K, Gros P, Housman DE, Fojo A, Shen DW, Gottesman MM, Pastan I (1986) Isolation of human mdr DNA sequences amplified in multidrug-resistant KB carcinoma cells. *Proc Natl Acad Sci USA* 83, 4538–4542

49 Schierenberg E (1988) Localization and segregation of lineage-specific cleavage potential in embryos of *Caenorhabditis elegans*. *Roux's Arch Dev Biol* 197, 282–293

50 Schierenberg E, Junkersdorf, (1992) The role of eggshell and underlying vitelline membrane for normal pattern formation in the early *C elegans* embryo. *Roux's Arch Dev Biol* 202, 10–16

51 Schulze-Gahmen U, Brandsen J, Heather DJ, Morgan DO, Meijer L, Vesely J, Kim SH (1995) Multiple modes of ligand recognition: crystal structures of cyclin-dependent protein kinase 2 in complex with ATP and two inhibitors, olomoucine and isopentenyladenine. *Proteins Structure Function Genetics*, in press

52 Schutte B, Reynders MMJ, Van Assche CLMVJ, Hupperets PSGJ, Bosman FT, Blijham GH (1987) An improved method for the immunocytochemical detection of bromodeoxyuridine labeled nuclei using flow cytometry. *Cytometry* 8, 372–376

53 Serrano M, Hannon GJ, Beach D (1993) A new regulatory motif in cell-cycle control causing specific inhibition of cyclin D/cdk4. *Nature* 366, 704–707

54 Shapiro H (1941) Centrifugal elongation of cells and some conditions governing the return to sphericity and cleavage time. *J Cell Comp Physiol* 18, 61–78

55 Sherr CS (1993) Mammalian G1 cyclins. *Cell* 73, 1059–1065

56 Someya A, Tanaka N, Okuyama A (1994) Inhibition of cell cycle oscillation of DNA replication by a selective inhibitor of the cdc2 kinase family, butyrolactone I, in *Xenopus* egg extracts. *Biochem Biophys Res Commun* 198, 536–545

57 Sulston JE, Schierenberg E, White J, Thomson JN (1983) The embryonic cell lineages of the nematode *Caenorhabditis elegans*. *Dev Biol* 100, 64–119

58 Th'ng JPH, Wright PS, Hamaguchi J, Lee MG, Norbury CJ, Nurse P, Bradbury EM (1990) The FT210 cell line is a mouse G2 phase mutant with a temperature-sensitive CDC2 gene product. *Cell* 63, 313–324

59 Van den Heuvel S, Harlow E (1993) Distinct roles for cyclin-dependent kinases in cell cycle control. *Science* 262, 2050–2054

60 Vaulot D, Olson RJ, Chisholm SW (1986) Light and dark control of the cell cycle of two marine phytoplancton species. *Exp Cell Res* 167, 38–52

61 Vaulot D, Partensky F, Neveux J, Mantoura RFC, Llewellyn C (1990) Winter presence of prochlorophytes in surface waters of the northwestern Mediterranean Sea. *Limnol Oceanogr* 35, 1156–1164

62 Vesely J, Havlicek L, Strnad M, Blow JJ, Donella-Deana A, Pinna L, Letham DS, Kato JY, Détivaud L, Leclerc S, Meijer L (1994) Inhibition of cyclin-dependent kinases by purine derivatives. *Eur J Biochem* 224, 771–786

63 Xiong Y, Hannon GJ, Zhang H, Casso D, Kobayashi R, Beach D (1993) p21 is a universal inhibitor of cyclin kinases. *Nature* 366, 701–704